

The Structural and Morphology of (La_{0.6}Sr_{0.4})MnO₃ Thin Films Prepared by Pulsed Laser Deposition

Hai Bin Yang^{1,a}

Department of Physics, college of Science Naval University of Engineering Wuhan, China

Abstract. (La_{0.7}Sr_{0.3})MnO₃ (LSMO) thin films were prepared on Si (100) substrate by pulsed laser deposition (PLD). Both structure and surface morphology of the films were investigated by X-ray diffraction (XRD) and atomic force microscopy (AFM). Furthermore, the chemical states and chemical composition of the films were determined by X-ray photoelectron spectroscopy (XPS) near the surface. The results indicate that the films grown on Si (100) substrates have a single pseudo cubic perovskite phase structure with a high (100) orientation. The XPS results show that La, Sr and Mn exist mainly in the forms of perovskite structure and a SrO layer was found on outermost surface.

1 Introduction

Due to the effect of colossal magnetoresistance (CMR), extensive studies have been carried out on (La_{1-x}Sr_x)MnO₃ (LSMO) for its interesting properties and potential application on various devices such as magnetic field sensors and memories [1-3]. LSMO shows good metallic phase with very low resistivity, moreover the electrical resistivity of LSMO can be controlled by varying the deposited oxygen pressure and remain stable against further thermal treatments in various oxygen pressure [4]. In recent years, increasing studies are being carried out on ferroelectric films and great interests have been triggered in some electronically conductive perovskite oxides [5-7]. Those conducting oxides materials showed many advantages including excellent conductivity like mental, overcoming fatigue in ferroelectric films, and with perovskite structure that is suitable for improving lattice match when they are employed as electrodes. As a material with conducting function, LSMO is also drawing more and more attention for its significant properties showing in fabrication of ferroelectric devices, in which LSMO was used as electrodes. It was reported that ferroelectric (Pb_{0.6}Ca_{0.4})TiO₃ and (Ba_{0.7}Sr_{0.3})TiO₃ thin films grown on LSMO films buffer layer showed excellent ferroelectric and fatigue properties comparing those with on other mental electrode [8-10]. There are a few reports about characters of LSMO films themselves, especially when they are employed as electrodes.

In this work, (La_{0.7}Sr_{0.3})MnO₃ films have been grown on single crystal substrate of Si (100) by pulsed laser deposition (PLD) process. We have used XPS and got a detailed knowledge of the surface chemical composition of (La_{0.7}Sr_{0.3})MnO₃ films. The purpose of the present paper is to study the crystal structure and identify the composition and chemical state of the surface of LSMO films prepared by PLD process.

2 Experimental

The LSMO thin films were grown on Si (100) substrates kept at 650°C by PLD using a KrF excimer pulsed laser ($\lambda=248$ nm), and LSMO target. The LSMO target was prepared by conventional solid state reaction [10-11]. The films were deposited at a laser repetition rate of 10 Hz and pulsed laser energy of 300 mJ. The base pressure of the system is 2 mTorr. The deposition time and rate are 10 min and 20 nm/min respectively. The oxygen pressure was kept at 200 mTorr. Finally, the LSMO films were crystallized in situ at 650 °C in 400 mTorr of oxygen for 10 min and cooled down slowly to room temperature. The thickness of the LSMO thin films measured by a Tencor P-10 surface profiler (KLA-Tencor Corporation, USA) was about 200 nm.

The crystalline structure of the LSMO thin films on Si (100) substrates were analyzed by a Philips PW3710 X-ray diffractometer. The resistivity of the LSMO thin films measured by a standard four-point method at room temperature is $6.4 \times 10^{-4} \Omega \cdot \text{cm}$. The surface morphology and

^a Corresponding author: 8895660@qq.com

roughness were determined by AFM using tapping mode amplitude modulation. To study the film surface, XPS analyses were carried out on the ESCALab250 (VG Scientific) spectrometer by using Mg Ka (1253.6 eV) radiation.

3 Results and Discussion

3.1 Structure and Surface morphology.

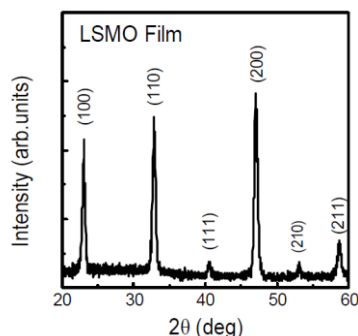


Figure. 1 XRD patterns of LSMO films

Fig. 1 shows the XRD patterns of the LSMO thin films on Si (100) substrates. From the XRD analysis for the LSMO films prepared by PLD process, six-peaks (100), (110), (111), (200), (210) and (211) were observed in the XRD patterns and these diffraction peaks can be indexed to LSMO phase with pseudo cubic perovskite structure. The relative peak intensity of $\Sigma I(h00)/\Sigma I(hkl)$ are found to be 0.588 for LSMO thin film on Si(100) substrates, indicating a remarkably strong (100) grain orientation. From the XRD data we estimated the lattice parameter to be 0.386 nm, which is equal to that of bulk ($a=0.387$ nm). Due to large lattice mismatch between LSMO films and Si ($a=0.543$ nm). Therefore, the high (100)-orientation of LSMO thin films on Si (100) substrate is considered to be a self-textured growth, which is in accordance with minimum surface energy conditions.

3.2 Composition.

Fig. 2 shows the wide-scan XPS spectrum of the LSMO thin film on Si (100) substrate in the binding energy range of 0-1100 eV. All of the binding energies at various peaks were calibrated by the binding of C 1s (284.60 eV) as shown in Fig. 3, the LSMO film contains La, Sr, Mn, O and C elements near its surface, and no other impurity element was detected in the spectrum up to 1100 eV except carbon. The carbon results from surface contamination. The quantitative atomic

composition near the film surface was determined from the XPS spectra of La 3d, Sr 3d, Mn 2p, and O 1s by using sensitivity factors of 10, 1.48, 2.6, and 0.66, respectively.

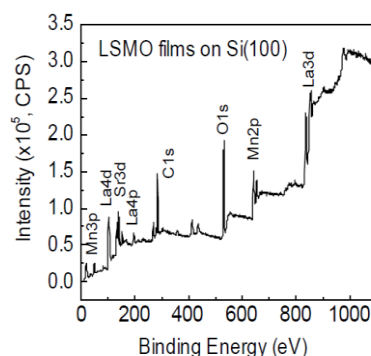
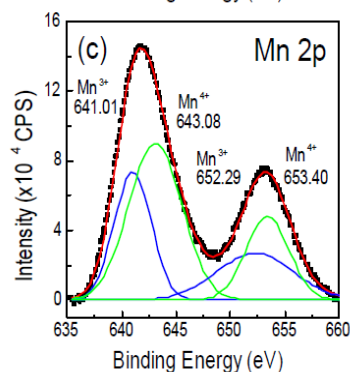
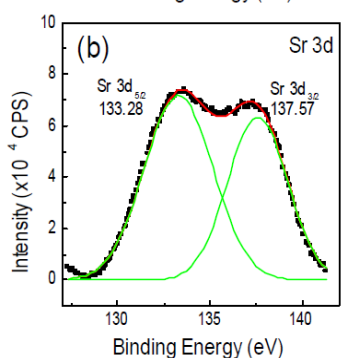
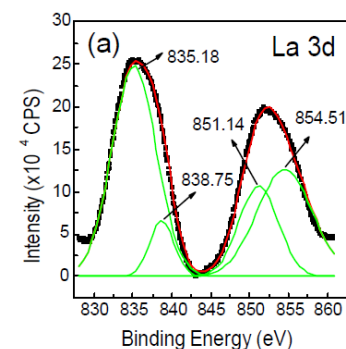


Figure. 2 Wide-scan XPS spectrum of the deposited on Si (100) substrate and LSMO thin film on Si (100) substrate crystallized in situ at 650°C for 10 min crystallized in situ at 650°C for 10 min.



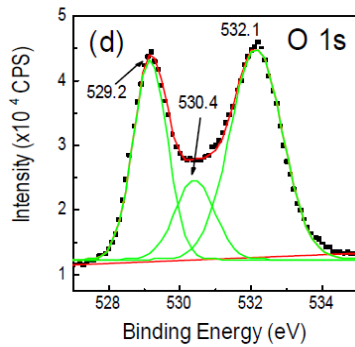


Figure. 3 Narrow-scan XPS spectra of (a) La 3d, (b) Sr 3d, (c) Mn 2p and (d) O 1s for the LSMO. The combined peaks were decomposed into individual components (red lines) on the assumption of a Gaussian line shape

Fig. 3 (b) shows the narrow-scan spectrum of Sr 3d and there are two peaks observed at 133.28 and 137.57 eV, respectively. The existing of Sr in LSMO films surface should be in the binding formation of SrO. We can infer that the main structure of LSMO surface should be perovskite structure that is able to offer suitable lattice match for preferred orientation. However, SrO is rocksalt structure with a lattice parameter of 0.516 nm that will induce so great lattice mismatch for BZT films that a preferred (100) orientation is impossible. Whereas, Bertacco et al. proved his mode with a conclusion that SrO is possible to form an epitaxial growth onto LSMO (001) with a 45° rotation of the surface square lattice of SrO with respect to that of LSMO, and the outermost SrO layer could be considered as a $\text{La}_{0.7}\text{Sr}_{0.3}\text{O}$ plane in which La has been completely substituted by Sr [12]. Therefore, It is reasonable to explain BZT films (with lattice parameter $a=0.405\text{nm}$) grown epitaxially on LSMO because there is a high similarity between SrO and $\text{La}_{0.7}\text{Sr}_{0.3}\text{O}$ plane that can offer a more suitable lattice parameter for BZT epitaxial growth.

Fig. 3 (c) illustrates the fine spectrum of Mn 2p core levels. After analyzed by Gaussfitted curve the spectrum are decomposed into two doublet peaks. The peak positions of Mn^{3+} and Mn^{4+} are observed at 641.01 and 643.08 eV, respectively for Mn 2p_{3/2} of LSMO. Also, the peak positions of Mn^{3+} and Mn^{4+} are observed at 652.29 and 653.40 eV, respectively for Mn 2p_{1/2} of LSMO. The value of 641.01 eV is close to the binding energy value 641.9 eV of the Mn 2p_{3/2} level in $\alpha\text{-Mn}_2\text{O}_3$ [13]. And the binding energies of Mn^{3+} and Mn^{4+} at 641.01 and 643.08 eV and close to that the value 641.3 and 642.8 eV of the Mn 2p_{3/2} level in $\text{La}_{2/3}\text{Sr}_{1/3}\text{MnO}_3$ composites [14]. As we known that La and Sr in LSMO compounds control and cause the mixed valence of Mn^{3+} and Mn^{4+} ions and CMR effect is attributed to the

itinerant electrons via $\text{Mn}^{3+}\text{-O-Mn}^{4+}$. In order to describe this mixed $\text{Mn}^{3+}/\text{Mn}^{4+}$ system.

Fig. 3 (d) represents an asymmetric peak of the O1s spectra and a doublet peaks were founded. The doublet peak agrees well with the reported data on alkaline earth substituted and unsubstituted ABO_3 type perovskites [15]. The asymmetric peak indicated that existing oxygen had more than one state. Analyzing with Gauss curve-fitting process, we can find the existence of three components at the O 1s spectra with three binding energies positions at 529.2, 530.4 and 532.1 eV, respectively. The lower binding energy (BE) 529.2 and 530.4 eV is always accepted as weakly bound oxygen-metal bonds in crystal lattice such as the presence of La-O and Mn-O oxide [16]. Similar O 1s XPS with shoulder, two peaks at 529.5 and 531.0 eV, were observed on $\text{La}_{0.5}\text{Sr}_{0.5}\text{MnO}_3$ powder compounded in literature [17], in which the 529.5 eV components was attributed to O^{2-} iron of metal oxide. It is reasonable to attribute the O 1s binding energy 532.1 eV to Sr-O bond for the existence of SrO_2 layer on the outermost surface of LSMO films.

4 Conclusions

In this paper LSMO film on Si (100) substrate was prepared by PLD process. The films show pseudo cubic perovskite structure with an orientation in (100) plane. Through AFM, the surface of LSMO films deposited on Si (100) was found to be smooth and dense. Based on the analysis of the XPS, elements like La, Sr, Mn and O that showed different states that respond to the perovskite structure and an outermost SrO layer was found. Simultaneity, C contamination was observed in the films.

References

1. N.TSUDA, K.NASU, A.FUJIMORI, K.SIRATORI: *Electronic Conduction in Oxides*, Springer, Berlin(2012)
2. H.TANAKA, T.KAWAI: *Solid State Commun Vol. 112* (1999), p. 201-205
3. M.SIRENA,N.HABERKORN, L.B.STEREN and J.GUIMPEL: *J. Appl. Phys Vol. 103* (2013), p. 6177-6181
4. W.B.WU, K.U. WONG, X.G. LI, C.L. CHOY and ZHANG YH: *J. Appl. Phys Vol. 97*(2010),p. 3006-3010
5. X.G. TANG, H.F. XIONG, L.L. JIANG and H.L. CHAN: *Cryst. Growth Vol.305*(2015), p. 613-619
6. I.D. KIM and H.G. KIM: *Jpn.J. Appl. Phys. Part 1 Vol. 50*(2011), p. 2357-2362

7. B. CHEN, H. YANG, J. MIAO, L. ZHAO, L.X. CAO, B. XU, X.G. QIU and B.R. ZHAO: J. Appl. Phys Vol. **107**(2015), 024106-1(4)
8. C.C. CHOU, C.S. HOU, G.C. CHANG and H.F. CHENG: Appl. Surf. Sci Vol. **1449**(2013), p. 413-417
9. J. MIAO, L. CAO, J. YUAN, W. CHEN, H. YANG, B. XU, X. QIU and B. ZHAO: J. Cryst. Growth Vol. **296** (2013), p. 498-506
10. S.H. Lim, M.Murakami, S.E.Lofland, A.J.Zambano, L.G.Salamanca-Riba and I.Takeuchi: Journal of Magnetism and Magnetic Materials Vol. **351**(2014), p. 1955-1958
11. S.Y. YANG, W.L. KUANG, Y. LIOU, W.S. TSE, S.F. LEE, Y.D. YAO: J. Magn. Magn. Mater Vol. **288**(2011), p. 326-331
12. R. BERTACCO, J.P. CONTOUR, A. BARTHELEMY and J. OLIVIER: Surf. Sci Vol. **511**(2002), p. 366-372
13. V.M. Petrov, M.I. Bichurin, V.V. Zibtsev, S.K. Mandal, and G. Srinivasan: JOURNAL OF APPLIED PHYSICS Vol. **116**(2014), 113901
14. Q.X. ZHOU, M.X. DAI, R.H. WANG, L. JIN, S.J. ZHU, L. QIAN, Y.M. WU and J.W. FENG: Physica B Vol. **391**(2012), p. 206-211
15. R.J. L, T.B. W, and Y.H. C: Scripta Materialia Vol. **59**(2014), p. 897-900
16. L.JING, Z. YI, L.Y. HUA, and C. W. NAN: JOURNAL OF APPLIED PHYSICS Vol. **105**(2013), 083915
17. J.P. ZHOU, W.ZHAO, Y.Y. GUO, P. LIU, and H.W. ZHANG: JOURNAL OF APPLIED PHYSICS Vol. **105**(2011), 063913